Applied Catalysis A: General 401 (2011) 56–64

Contents lists available at ScienceDirect

Applied Catalysis A: General

journal homepage: www.elsevier.com/locate/apcata

Selective hydrogenation of citral over Pt/KL type catalysts doped with Sr, La, Nd and Sm

J. Álvarez-Rodríguez[b,c], I. Rodríguez-Ramos[a,c], A. Guerrero-Ruiz[b,c], A. Arcoya[a,c,*]

[a] Instituto de Catálisis y Petroleoquímica. CSIC, C/Marie Curie n° 2, Madrid 28049, Spain
[b] Dpto. Química Inorgánica y Técnica, UNED, Senda del Rey n° 9, Madrid 28040, Spain
[c] Grupo de Diseño y Aplicación de Catalizadores Heterogéneos, Unidad Asociada UNED-ICP (CSIC), Spain

ARTICLE INFO

Article history:
Received 11 January 2011
Received in revised form 27 April 2011
Accepted 28 April 2011
Available online 6 May 2011

Keywords:
Pt/KL catalysts
Selective hydrogenation
Citral
Geraniol
Nerol, Promoters, Sr, La, Nd, Sm

ABSTRACT

The effect of Sr and some lanthanides (La, Nd, Sm) as promoters of Pt/KL supported catalysts is analyzed in the selective hydrogenation of citral in the liquid phase. Characterization of the catalysts by XRD, N_2 adsorption, H_2 chemisorption, TPD of NH_3, XPS and competitive hydrogenation of benzene/toluene mixtures shows that impregnation of KL zeolite with $Sr(NO_3)_2$ in aqueous solution, followed by calcination prior to the incorporation of Pt, increases the surface basicity of the zeolite, which hinders the dispersion of Pt and promotes the formation of electron-rich platinum nanoparticles ($Pt^{\delta-}$). Ion exchange of K^+ by rare earth cations (La^{3+}, Nd^{3+} and Sm^{3+}) increases the surface acidity of the zeolite and favors the dispersion of Pt, but with preferential location at the external surface of the zeolite. Furthermore, acidity promotes the formation of electron-deficient metal species ($Pt^{\delta+}$). Catalytic performances for the citral hydrogenation at 323 K and 5 MPa show that strontium addition enhances the hydrogenation activity of Pt, thus favoring the formation of citronellol as main reaction product (S = 80%) and increasing the yield to geraniol and nerol. Lanthanides as countercations diminish the overall hydrogenation activity of Pt/KL catalysts, but improve their selectivity towards unsaturated alcohols. Selectivity towards the reaction products is related to the mode and strength of the electronic interactions of the conjugated unsaturated bonds of citral reactant molecules with the metal surface species Pt^0, $Pt^{\delta+}$ or $Pt^{\delta-}$ on the zeolite.

1. Introduction

Selective hydrogenation of α,β-unsaturated aldehydes is one of the more important reactions in the industry. Among these compounds, citral (3,7-dimethyl-2,6-octadienal) is an interesting probe molecule because it presents two unsaturated conjugated bonds, C=C and C=O, as well as an isolated C=C bond. The conjugated bonds can be selectively hydrogenated either into unsaturated alcohols (hydrogenation of the C=O bond) or into citronellal (hydrogenation of the conjugated C=C bond), following parallel routes, as shown in the generally accepted reactions network given in Fig. 1. Subsequent hydrogenation of the C=O bond of citronellal and the C=C bond of geraniol and nerol yields citronellol and, thereafter, 3,7-dimethyloctanol. All these products are important perfumery chemicals, furthermore, nerol and geraniol are specially valuable because they are also used as intermediates in the synthesis of expensive fine chemicals, vitamins and polymers of special properties [1]. In the complex set of reactions involved in this process, formation of unsaturated alcohols is less favored than that of citronellal [2] but it may be improved by using metal catalysts with an adequate formulation and working under optimized experimental conditions [3,4]. In this sense, it has been demonstrated that incorporation of electron-acceptor additives to Pt supported catalysts enhances selectivity towards alcohols in the hydrogenation of cinnamaldehyde [5]. Likewise, Co improves the selectivity towards geraniol and nerol from citral over Pt supported catalysts [6] and Ni, Co and Fe that of crotyl alcohol from crotonaldehyde over Pt/SiO_2. Ga, Ge and Sn increase the selectivity towards crotyl alcohol [7], while Ge promotes formation of unsaturated alcohols from citral over Rh and Pt supported on TiO_2 [8,9]. In other cases, Fe, Sn and Ge were used with this aim in the preparation of platinum and ruthenium catalysts for other reactions [10–14]. On the other hand, the use of electron-donor additives and supports of different natures have been also proposed in order to favor the hydrogenation of carbonyl group in α,β-unsaturated aldehydes [3,4].

In comparison with amorphous materials, the use of zeolites as catalyst support for the selective hydrogenation of α,β-unsaturated aldehydes is more attractive, due to the fact that the three-dimensional structure of channels and cavities of some of them can play a favorable role in order to improve the selectivity towards the unsaturated alcohols. Gallezot et al. [15–17] studied the hydro-

* Corresponding author at: Instituto de Catálisis y Petroleoquímica, Marie Curie, n° 2, 28049 Madrid, Spain. Fax: +34 915854760.
E-mail address: aarcoya@icp.csic.es (A. Arcoya).

0926-860X/$ – see front matter © 2011 Elsevier B.V. All rights reserved.
doi:10.1016/j.apcata.2011.04.045

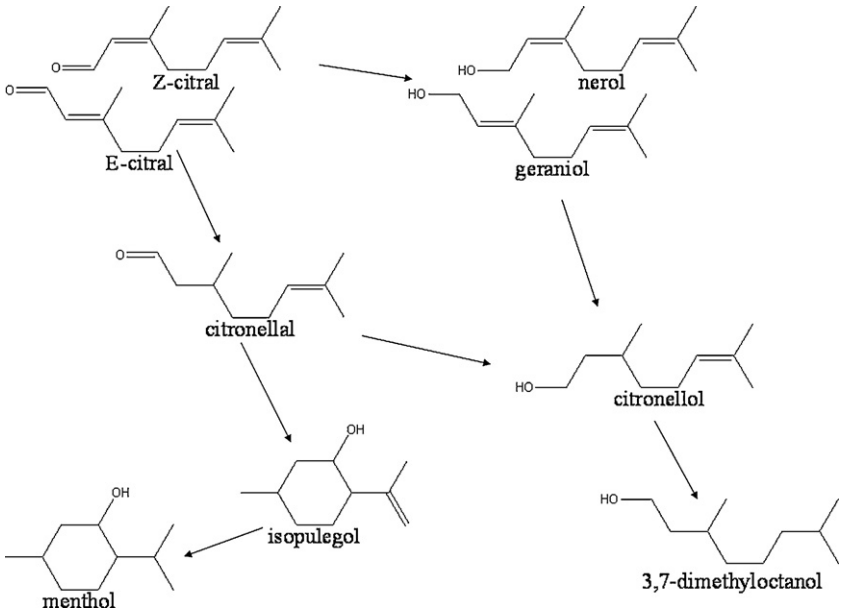

Fig. 1. Reaction networks for the hydrogenation of citral in the liquid phase at 323 K and 5 MPa.

genation of cinnamaldehyde over transition metals supported on Y and beta zeolites and found an enhancement of the selectivity towards cinnamyl alcohol. They attributed the results to the preferential hydrogenation of the terminal C=O group of cinnamaldehyde, which is forced by the pore structure of the Y-zeolite and by large metal particles inside the beta zeolite. Likewise, the high selectivity towards geraniol from geranial over Pt/β-zeolite, observed by Tas et al. [18] was explained in terms of end-on adsorption of the aldehyde molecule on the metal clusters. Enhanced selectivity towards unsaturated alcohols over Ru/MCM-41 catalysts has also been reported [19,20]. In a similar way, the higher activity and selective towards cinnamyl alcohol from cinnamaldehyde over Pt/KL catalysts, in comparison with that obtained over Pt/Al_2O_3 [21], was attributed to the channels structure and basicity of the KL zeolite and to the morphology of the supported metal particles.

Recent works by our research group devoted to the hydrogenation of citral in the liquid phase over Ru/KL catalysts [22–24] showed the effect of several properties of the catalyst on the selectivity of the reaction, namely, the framework structure and basicity of the zeolite, the steric hindrances by metal particles inside of pores and electron transfers in bimetal particles. The role of the deactivation by the reaction products or by thiophene on the selectivity has been also analyzed [25]. Now, aiming to improve the selectivity towards unsaturated alcohols of Pt/KL catalysts in the hydrogenation of citral, the effect of either electron-acceptor additives (La^{3+}, Nd^{3+}, Sm^{3+}) or an electron-donor one (SrO) on the performance of these catalysts, is analyzed and discussed. The former were incorporated to the zeolite as countercations, while strontium is present as an extra-framework additive.

2. Experimental

2.1. Catalysts preparation

A KL-zeolite (Union Carbide, SK-45, $K_9Al_9Si_{27}O_{72}$ in atoms per unit cell and average particle size between 53 and 65 μm) calcined at 873 K for 4 h, was used as catalysts support. The catalysts were prepared as follows.

Sample PtKL. Platinum (1 wt%) was incorporated to the zeolite by the incipient wetness impregnation method, by using an aqueous solution of $Pt(NH_3)_4(OH)_2$ as metal precursor. No chlorinated precursor of platinum was used in order to avoid side reactions.

Samples PtLaKL, PtNdKL and PtSmKL. Different portions of the zeolite were ion exchanged with nitrates of La, Nd or Sm, respectively, in aqueous solution. The cation content in these solutions was twice that corresponding to the exchange capacity of the zeolite. The operation was carried out by adding, dropwise, 200 mL of one of these solutions to a suspension containing 20 g of zeolite into 400 ml of distilled water, under stirring at reflux temperature. After 24 h of treatment, the suspension was filtered and the powder successively washed with distilled water to remove occluded ions, dried at 393 K and calcined at 873 K for 8 h. These samples were subsequently impregnated with $Pt(NH_3)_4(OH)_2$ aqueous solution, as indicated above.

Sample PtSrKL. A portion of zeolite was impregnated with 2 wt% of Sr, from a $Sr(NO_3)_2$ aqueous solution. After drying at 393 K, decomposition of the precursor was made by calcination at 873 K for 3 h and afterwards platinum was incorporated following the procedure above mentioned.

After incorporation of the metal precursor, all the samples were successively dried at 393 K, calcined under flowing oxygen at 573 K and finally, in order to assure complete reduction of Pt, they were treated under flowing H_2 at 773 K for 3 h and stored in the absence of air for subsequent use.

2.2. Catalysts characterization

Chemical composition of the catalysts was determined by inductively coupled plasma-atomic emission (ICP-AES), while crystallinity of the zeolite was checked by XRD in a Seifert C-3000 powder diffractometer, using Cu Kα radiation at 40 mA and 40 kV, with slits of 1° and 0.1°. Specific surface area was determined by application of the BET method to the isotherm of N_2 adsorption at 77 K obtained in a Micromeritics Asap 2000 system.

Metal dispersion of the catalysts was calculated from the hydrogen chemisorption measurements performed in a volumetric apparatus at 298 K. A reduced and outgassed sample of catalyst (0.25 g) was contacted with successive hydrogen pulses in the pressure range 5–40 kPa, whereas the loss of pressure was measured. The hydrogen consumption to form the monolayer was calculated by extrapolating to zero pressure the linear portion of the adsorp-

Table 1
Chemical composition, specific surface area and metal dispersion of the catalysts.

Catalyst	K^+ (wt%)	Me (wt%)	IE (%)	Pt (%)	S_A ($m^2\ g^{-1}$)	D (%)
KL	11.9				245	
PtKL	11.8			0.95	220	42
PtSrKL	11.8	1.9		0.96	122	23
PtLaKL	8.9	3.4	25.2	0.93	169	61
PtNdKL	9.2	3.2	21.8	1.04	115	69
PtSmKL	10.0	2.3	16.0	0.94	111	66

Me: Sr, La, Nd or Sm; IE: ion exchange degree of rare earth cation; S_A, BET surface area; D, platinum dispersion.

tion isotherm. The number of exposed metal atoms was calculated assuming an atomic stoichiometry H/Pt = 1/1 atom/atom. Average metal particle size was estimated assuming the spherical model of particle.

Surface acidity of the samples was measured by temperature programmed desorption (TPD) of NH_3 in a conventional flow system apparatus. In this case the outgassed catalyst sample (0.5 g) was saturated with pulses (1 mL) of NH_3 at RT and subsequently stabilized at 373 K under helium stream and heated from 373 K to 823 K at 10 K min^{-1}. The desorbed NH_3 was collected with a 0.01 M HCl solution and afterwards titrated by using a 0.01 M NaOH solution.

Basicity of some selected samples was evaluated by CO_2 chemisorption in the same volumetric apparatus used for hydrogen adsorption measurements. The catalyst samples, previously reduced and outgassed, were contacted at run temperature with successive pulses of CO_2 in the pressure range 0–30 kPa, while the loss of pressure was measured. The CO_2 uptake was determined extrapolating to zero pressure the linear portion of the adsorption isotherm.

Surface of the catalysts was analyzed by X-ray photoelectron spectroscopy (XPS) with an Omicron Spectrometer equipped with an EA-125 hemispherical electron multichannel analyzer and a MgKα X-ray source having a radiation energy of 1253.6 eV. Samples of the reduced catalysts (0.2 mg) mounted on the sample holder and introduced into the chamber were successively outgassed, treated under H_2 (10%)/Ar flow for 2 h at 673 K and outgassed for 6–8 h, in order to achieve a dynamic vacuum below 10^{-8} Pa. Spectra were registered at 150 W and a pass energy of 50 eV. The electronic state of Pt was characterized by the binding energy of the $4f_{5/2}$ peak, employing as internal reference that of the Si 2p peak (103.5 eV).

In order to evaluate the overall electronic state of supported platinum from a chemical point of view, the catalysts were tested in the competitive hydrogenation of toluene/benzene mixtures, following the method by Tri et al. [26]. Experiments were performed in a conventional flow reactor with 0.5 g of catalyst, at 373 K and atmospheric pressure. The benzene and hydrogen pressures did remain constant, while that of toluene was modified in the range 1.9–9.6 kPa. The total flow was 125 $cm^3\ min^{-1}$ and the conversion was always lower than 10%. Prior to the reaction, the reduced catalyst was successively outgassed and treated at 723 K under flow of hydrogen for 30 min in order to assure complete removal of adsorbed oxygen, if any. Reaction products were analyzed on line in a FID chromatograph.

2.3. Catalytic activity measurements

Catalytic performance of the samples in the hydrogenation of citral in the liquid phase, was studied in a reactor operated in batch mode (Autoclaves Engineers) under stirring (500 rpm) at 323 K and 5 MPa. The catalyst samples reduced "ex situ" (0.5 g) were suspended in 40 mL of 2-propanol under inert atmosphere and then transferred to the reaction flask containing a mixture of 0.5 mL of citral and 60 mL of 2-propanol. After outgassing under helium flow, the temperature was risen at 323 K, helium substituted by hydrogen and the pressure adjusted at 5 MPa. This was considered to be the time zero of the run and successive samples of the reacting mixture were periodically taken and analyzed by gas-chromatography. Previously it was probed that under the reaction conditions used the reactor operates under kinetic/catalytic control, with negligible mass transfer limitations [27].

3. Results and discussion

3.1. Catalysts characterization

Table 1 summarizes the chemical composition, BET surface area and metal dispersion of the catalysts. As shown, the platinum loading is practically coincident with the one theoretically incorporated into the samples (1 wt%) while the low ion exchange degrees (IE) obtained for lanthanide ions (16–25%) seem to be those corresponding to the thermodynamic equilibrium, according to the potentiometric measurements performed during the preparation of the samples. On the other hand, these latter values are consistent with the fact that only the open cation positions (C and D sites) of the four positions of the KL zeolite are directly exchangeable [28]. With regard to the sample PtSrKL, the strontium loading was that expected.

The X-ray diffraction patterns of the samples, no shown for sake of simplicity, were very similar to that of the raw zeolite and in coincidence with the one previously reported by Tracy et al. [29] for Linde type L zeolite (LTL). Only the diffraction patterns of samples containing rare earth showed small variations in the angles of diffraction of the zeolite, which could be attributed to changes in the lattice parameters caused by the partial ion exchange of K^+, rather that to changes of crystallinity. For PtSrKL, the absence of reflexions additional to those characteristic of KL zeolite suggests that strontium is highly dispersed on the support. On the other hand, data in Table 1 show a reduction of specific surface area for all the doped samples when comparing with that of PtKL, which may be attributed to a partial blockage of the zeolite channels.

It is important to note that the partial substitution of K^+ by La^{3+}, Nd^{3+} or Sm^{3+} in the zeolite framework increases the platinum dispersion (D) from 42% to 61–69%, which is in parallel with the values of the polarizing power of the countercations (Φ) given in Table 2. Polarizing power, which is the ratio between the cation charge and the ionic radius (Å), provides information about the electron-acceptor capacity of the cation in its close vicinity. In contrast with the rare earth cations, strontium diminishes the plat-

Table 2
Effect of the additives on the surface properties of the catalysts.

Catalyst	Φ	A (μEq $NH_3\ g^{-1}$)	$K_{Tol/Bz}$
PtKL	0.75	<20	1.86
PtSrKL		<20	0.93
PtLaKL	2.75	201	3.59
PtNdKL	2.77	258	3.67
PtSmKL	2.88	221	3.75

φ, ionic potential of the countercation = cation charge/ionic radium (Å); A, acidity of the catalyst; $K_{Tol/Bz}$, ratio of the adsorption coefficients of toluene and benzene in the hydrogenation of toluene/benzene mixtures.

Table 3
XPS analysis of the catalysts surface.

Catalyst	$Pt4f_{5/2}$ BE (eV)	Pt/Al (atom/atom)		Me/Al (atom/atom)	
		XPS	Bulk	XPS	Bulk
PtKL	74.5	0.0174	0.0136		
PtSrKL	74.3	0.0152	0.0137		0.0600
PtLaKL	75.4	0.0291	0.0133	0.0417	0.2520
PtNdKL	75.2	0.0339	0.0148	0.0339	0.2191
PtSmKL	74.8	0.1656	0.0134	0.0144	0.1590

Me: Sr, La, Nd or Sm.

inum dispersion to 23% in PtSrKL. In this case, because strontium nitrate was incorporated to the zeolite by impregnation, it is reasonable to assume that upon calcination at 873 K it was mainly transformed into SrO which, due to its basic character, seems to hinder the anchoring of platinum, thus favoring the formation of larger platinum particles.

Although the polarizing power is an important physicochemical characteristic of the isolated cation, the overall effect of the countercations in the catalyst is more rigorously represented by the surface acidity. This is also a measurable property related to the polarization strength, but strongly conditioned by the concentration, location and mobility of the countercations, among others. The acidity values (A) measured by TPD of ammonia (Table 2) range from 258 μEq NH_3 g^{-1} to <20 μEq NH_3 g^{-1}, following the sequence PtNdKL > PtSmKL > PtLaKL > PtKL ≈ PtSrKL. Since chemisorption of NH_3 over PtKL and PtSrKL was practically negligible, CO_2 chemisorption capacity of these samples was measured aiming to detect differences of basicity among them. Although CO_2 chemisorption is not a selective method to measure basic sites, it is expected that the quantitative difference of gas chemisorbed over both samples is only due to the effect of SrO in the latter. If it is so, the values of basicity obtained for PtKL and PtSrKL, 128 and 156 μmol g_{cat}^{-1}, respectively, indicate that strontium species provides an additional basic character to the KL zeolite and, therefore, an electron transfer from the basic sites of the support to platinum nanoparticles may be expected.

More insights on the chemical state of the surface of the catalyst were obtained by XPS analysis. Table 3 shows the binding energies of Pt and the surface atomic ratios. Due to the fact that the more intense signal of the doublet of Pt4f overlaps with the one of Al2p, the binding energy corresponding to $Pt4f_{5/2}$ was taken to characterize the surface state of platinum. The $Pt4f_{5/2}$ BE for PtKL and PtSrKL (74.5 and 74.3 eV) are close to that corresponding to Pt^0 (74.4 eV), whereas those for samples containing rare earth, in the range 74.8–75.4 eV, are higher than the characteristic value for Pt^0, but much lower than that of Pt^{2+} (around 76.6 eV), thus indicating the presence of electron-deficient species outside the zeolite, as a result of the interaction of the platinum nanoparticles with the electron-acceptor sites at the surface. On the other hand, comparison of the Pt/Al surface atomic ratios from XPS with the corresponding bulk atomic ratios, also summarized in Table 3, indicates that platinum is reasonably well distributed in PtKL, in contrast with the catalysts containing rare earth, where platinum is preferentially deposited on the external surface of the zeolite. This finding, together with the results of BET surface area, suggests that lanthanides, which are located mainly inside the zeolite, hinder the access of Pt to the zeolite channels in the order La < Nd < Sm, thus favoring the deposition of the metal on the outer surface of the support. Preferential deposition of Pt outside the zeolite in lanthanide doped catalysts was previously suggested from TPR measurements [30].

For PtSrKL the value of the XPS Pt/Al atomic ratio, which is very similar to that of the bulk ratio, indicates that strontium induces a homogeneous distribution of Pt in the zeolite framework. This observation suggests that a metal surface as low as that corresponding to 23% dispersion, cannot be attributed to metal particles of 4.7 nm of average size, because such value is much higher than the dimensions of cavities of the zeolite (0.48 nm × 1.24 nm × 1.07 nm). The low H_2 chemisorption capacity found for this sample could be rather attributed to the fact that a number of platinum nanoparticles of adequate size and shape may block part of the zeolite channels, thus occluding a fraction of the metal loading. This assumption was confirmed by TEM-XEDS analysis because, as it can be seen in Fig. 2, this sample exhibits a homogeneous distribution of platinum nanoparticles much smaller than the average particle size calculated from the H_2 chemisorption measurements. It is noticeable, on the other hand, that analysis by XEDS of PtSrKL displayed weak but constant signals of Sr in all the zones of the field analyzed, which induces to assert that Sr is highly dispersed and well distributed in the zeolite framework.

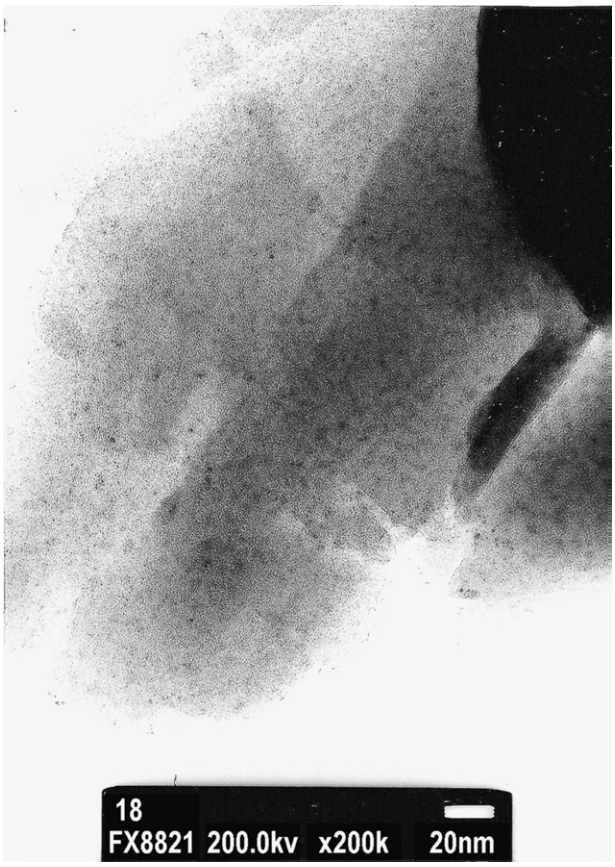

Fig. 2. Representative micrograph of PtSrKL catalyst.

Complementary information about the overall electronic state of platinum, involving species located outside and inside the zeolite, can be drawn from the competitive hydrogenation of benzene/toluene mixtures. In this system, because the ionization energy of toluene (8.82 eV) is lower than that of benzene (9.25 eV) the former will be preferentially adsorbed on the more electrophilic metal sites, thus hindering the adsorption of benzene [31,32]. For these competitive reactions, the ratio of the adsorption coefficients of toluene and benzene ($K_{Tol/Bz}$ in Table 2) obtained from the relative hydrogenation rates of each one of the reactants in the mixtures, is a very sensitive thermodynamic function of the electronic state of the Pt particles in the catalyst [33]. In short, with this method the higher the electron density of the metal the lower the $K_{Tol/Bz}$ value. The findings arising from analysis of the $K_{Tol/Bz}$ values, in Table 2, agree with those obtained from XPS analysis. Therefore, we can assert that the higher electron density of Pt clusters in the

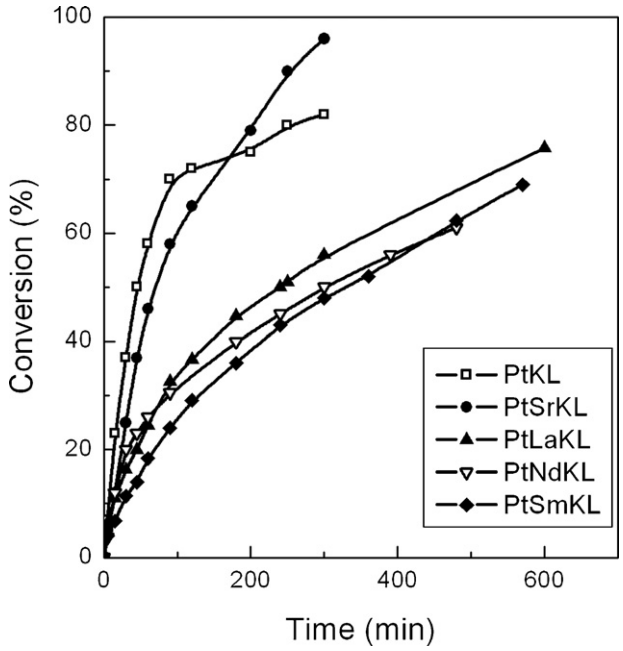

Fig. 3. Conversion of citral over the catalysts as a function of the reaction time, at 323 K and 5 MPa.

Sr-promoted catalyst is due to the higher basicity derived from the well distributed SrO species inside of channels, which interact with platinum particles, either directly or through the O^{2-} anions of the lattice. On the other hand, the electron-deficient species in catalysts doped with rare earth are originated by the interaction of Pt nanoparticles with the electron-acceptor sites at the surface in the close proximity [34,35], i.e. the Brönsted acid sites generated by hydrolysis of hydrated countercations, as indicated by Eq. (1).

$$n\mathrm{Pt}^0 + \mathrm{H}^+ \rightarrow [\mathrm{Pt}_n\mathrm{H}]^+ \quad (1)$$

The detection of $[Pt_nH]^+$ species, or simply $Pt^{\delta+}$, in similar catalysts to those used in this work, was already verified by the CO/FT-IR bands at wavenumbers above 2080 cm^{-1}, which were more intense in the catalyst doped with rare earth than in PtKL [30]. For PtSrKL, the absence of absorption bands at such wavenumbers in the corresponding CO/FT-IR spectrum (no included) together with the observation of bands at 2000 cm^{-1} and at lower wavenumbers, confirm the presence of small particles of Pt inside the channels, with an electronic structure strongly perturbed by the basic surrounding of the zeolite [36].

3.2. Hydrogenation of citral

Conversions of citral versus time at 323 K and 5 MPa for all the catalysts are depicted in Fig. 3. Initial activity (a_0) and *TOF*, calculated from the slope of these plots at initial time, are given in Table 4 together with selectivity towards the major reaction products, citronellal, geraniol and nerol, citronellol and 3,7-dimethyloctanol at 60% conversion level. Selectivity towards a product *i* (S_i) is defined as the number of citral molecules converted into *i* per 100 molecules of citral transformed. Formation of isopulegol, by isomerization of citronellal, was only observed over the most acidic sample PtNdKL, while either menthol or acetals were never observed.

As it can be seen, PtKL is initially the most active hydrogenation catalyst ($a_0 = 1.24\ \mu mol\ g^{-1}\ s^{-1}$) and, furthermore, its initial activity remains up to around 60% conversion (X). However, at higher conversions it strongly declines, being $0.20\ \mu mol\ g^{-1}\ s^{-1}$ for $X > 75\%$. Sample PtSrKL is initially less active than PtKL ($a_0 = 0.74\ \mu mol\ g^{-1}\ s^{-1}$) but, in contrast, its activity decreases only gradually in all range of conversions, without any dramatic change. As a consequence of such behavior the overall hydrogenation activity of PtSrKL is higher than that of PtKL at reaction times above 170 min. Catalysts containing rare earth are less active than PtKL, their respective initial activities being in the range 0.65–0.37 $\mu mol\ g^{-1}\ s^{-1}$. Furthermore, activity of these three catalysts considerably decays after 100 min of reaction, in particular that of PtNdKL, when only 35% conversion is reached.

Although deactivation of catalysts is not easily detected in liquid phase batch reactions, very prominent changes in the slope of the conversion versus time curves for the hydrogenation of α,β-unsaturated aldehydes, as those observed in Fig. 3 for several catalysts, have been considered to be a signal of deactivation of the active surface [19,37,38]. In a previous work, activity decay for Ru/KL type catalysts was already observed [39] and, since no loss of Pt was observed in the samples, it was attributed to the partial blockage of hydrogenation active sites by the reaction products of decarbonylation and/or oligomerization of citral, as suggested in other cases [40,41]. If one correlates the acidity values of the catalysts in Table 2 and the corresponding activity decay observed in Fig. 3, it is seen that the greater surface acidity, the higher decay of activity, in agreement with the well known fact that those undesirable reactions are favored on acid sites. In addition, the fact that the major part of Pt in the lanthanide doped catalysts is on the external surface of the zeolite, where the metal surface is more vulnerable to the effects of poisons, contributes to the early deactivation of these catalysts. On the contrary, the highest stability of the catalyst PtSrKL may be reasonably attributed to both the basic character of strontium oxide that neutralizes acid sites, and the fact that platinum nanoparticles are mainly located inside the zeolite. For PtKL, it is probable that deposition/adsorption of undesirable products on a number of metal nanoparticles of adequate size and shape, located at the pore mouth (0.71 nm diameter), gradually decreases the effective diameter of the zeolite channels in such a way that, after around 100 min of reaction, part of the metal sites are not any more accessible to the citral molecules. So that, from this moment the hydrogenation activity of this sample dramatically decreases.

Results in Table 4 show that PtKL and PtSrKL exhibit a very similar hydrogenation *TOF* (0.057 and 0.063 s^{-1}, respectively). However, the former is very selective towards citronellal ($S_{Cal} = 61\%$) while the further leads the reaction towards citronellol chiefly ($S_{Col} = 82\%$), with an important improvement of selectivity towards unsaturated alcohols ($S_{G+N} = 15\%$). This means that SrO, in addition to the inhibition of poisoning, induces changes in selectivity of platinum for the hydrogenation of citral, which are related to the presence of electron-enriched platinum species

Table 4
Activity and selectivity of the catalysts in the hydrogenation of citral at 323 K and 5 MPa.

Catalyst	PtKL	PtSrKL	PtLaKL	PtNdKL	PtSmKL
a_0 ($\mu mol\ g^{-1}\ s^{-1}$)	1.240	0.740	0.440	0.650	0.370
TOF (s^{-1})	0.057	0.063	0.014	0.018	0.011
S_{G+N}	6	15	26	33	32
S_{Cal}	61	3	44	35	40
S_{Col}	26	82	19	20	13

a_0, initial activity; S_{G+N}, selectivity towards geraniol + nerol; S_{Cal}, selectivity towards citronellal and S_{Col}, selectivity towards citronellol, at 60% conversion.

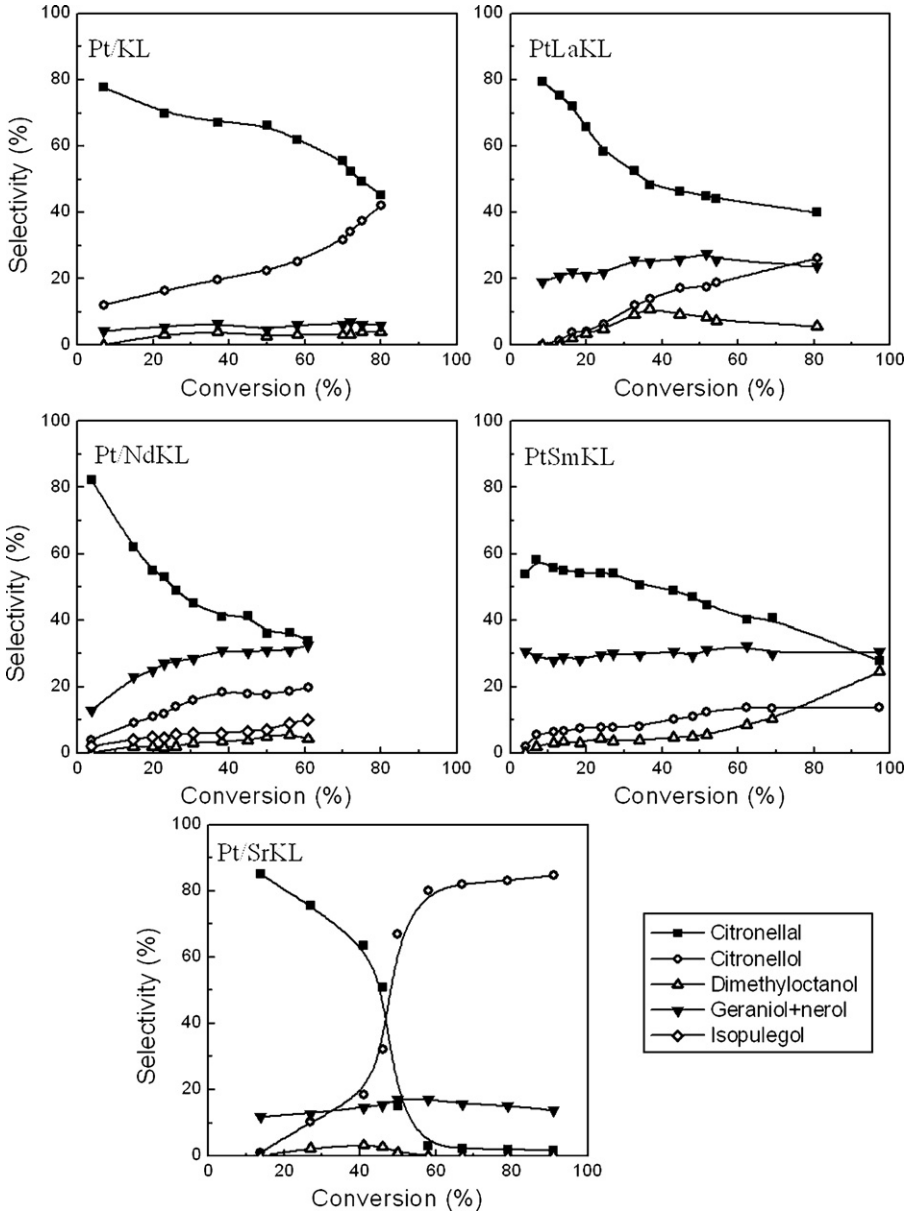

Fig. 4. Selectivity towards the reaction products as a function of the conversion at 323 K and 5 MPa.

($Pt^{\delta-}$) at the catalyst surface. For samples containing rare earth, where electron-deficient platinum species ($Pt^{\delta+}$) were evidenced, the *TOFs* are much lower than that of PtKL, while the respective selectivities towards the valuable unsaturated alcohols are remarkably enhanced, reaching 26% for PtLaKL and 33–32% for PtNdKL and PtSmKL.

A more complete analysis about the effect of strontium and rare earth on the performances of these catalysts can be drawn from the selectivity plots in Fig. 4. All the catalysts exhibit selectivity towards citronellal (S_{Cal}) higher than 60% at the beginning of the run, which decreases as the citral conversion increases. Thus, for PtKL, S_{Cal} diminishes from 75%, initially, to 45% in favor of citronellol (S_{Col}), while selectivity towards geraniol + nerol (S_{G+N}) remains around 6% in all the range of conversions analyzed. For lanthanide doped samples, evolution of S_{Cal} and S_{Col} are roughly comparable to those of PtKL, although the extent of the transformation of citronellal into citronellol is much lower. With respect to unsaturated alcohols, selectivity is significantly enhanced, reaching around 28% for PtLaKL and 32% when either Nd or Sm is incorporated to the zeolite. For PtSrKL, S_{Cal} abruptly diminishes from 85% to 3% at only 58% conversion, in favor of citronellol. In contrast, S_{G+N} is about 13–17% in the whole range of conversions. All the selectivity values we have obtained are consistent with the fact that hydrogenation of the conjugated C=C double bond of citral is thermodynamically and kinetically preferred to that of the C=O group [2] and with the experimentally demonstrated assertion by Singh et al. [42] that unsaturated alcohols are more stable intermediates than citronellal. On the other hand, it is clear that lanthanides as well as strontium enhance the selectivity towards unsaturated alcohols of the parent catalyst, PtKL.

Comparison of our kinetic results with those reported by other authors for this reaction is not immediate due to the important differences in the formulation of the catalysts and in the experimental conditions used, namely, metal loading, metal precursor nature, metal dispersion, solvents, temperature and pressure of reaction, among other experimental parameters which affect the overall reaction rate and selectivity. Even so, evolution of selectivities with conversion, given in Fig. 3 is, at least, comparable to those observed

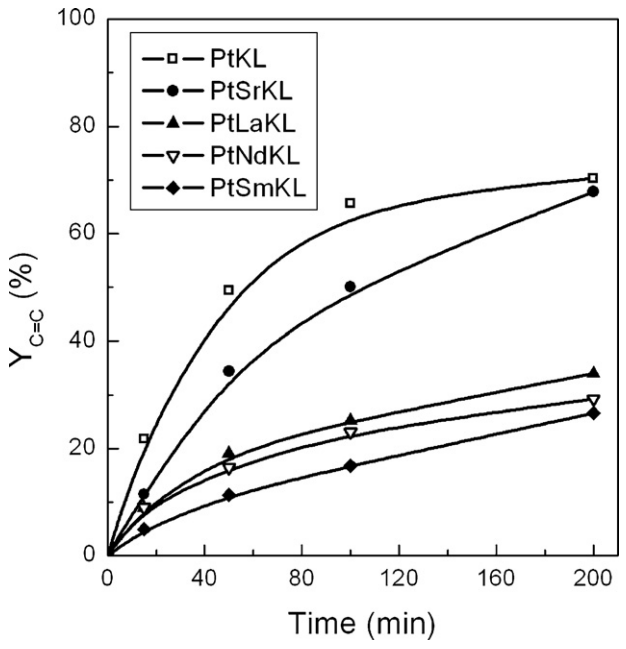

Fig. 5. Activity of the catalysts for hydrogenation of the conjugated C=C double bond of citral. $Y_{C=C}$: yield to citronellal + derivatives of citronellal.

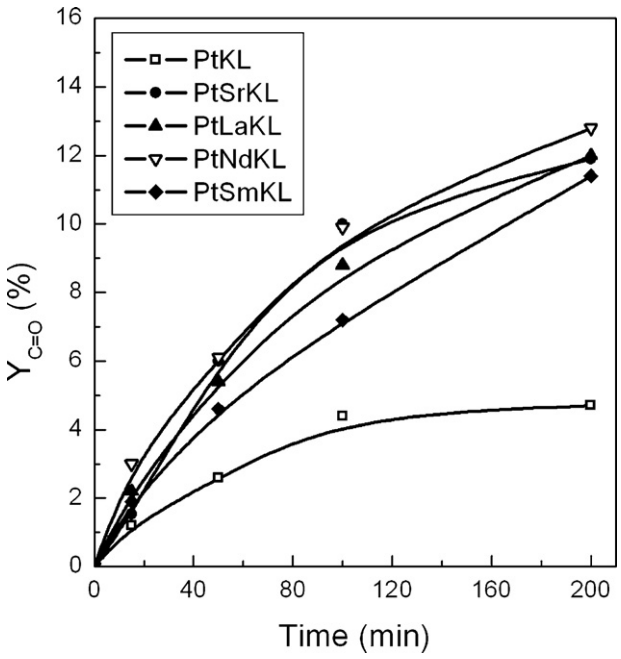

Fig. 6. Activity of the catalysts for hydrogenation of the C=O group of citral. $Y_{C=O}$: yield to geraniol + nerol.

by other authors using Pt/SiO_2 [43], Pt/carbon [44], Pt/Al_2O_3 [41] and Pt/nanocomposites [45] as catalysts. It is opportune to mention that separate experiments performed with catalysts prepared with different materials as supports showed that, under our standard reaction conditions, selectivity towards geraniol and nerol over KL catalysts is higher than those exhibited by catalysts prepared with graphite, zirconia or SiO_2 as support. On the other hand, we like to remind that enhancement of selectivity with conversion in favor of geraniol and nerol, as observed for PtNdKL, was already noticed for a Ru/KL catalyst [39] and attributed to the partial blocking of metal sites during the reaction by strongly adsorbed species that prevents adsorption of the conjugated C=C double bond and forces the adsorption end-on C=O group of citral.

Additional information about the kinetic effect of the rare earth and Sr in these catalysts is supplied by Figs. 5 and 6, where the yields to the hydrogenation products, grouped by families, are depicted. $Y_{C=C}$ groups the yields to the products successively formed via hydrogenation of the conjugated C=C double bond of citral (citronellal, citronellol, 3,7-dimethyloctanol and isopulegol) while $Y_{C=O}$ includes the yields to products arising from citral via hydrogenation of the carbonyl group, essentially geraniol and nerol. Yield to a reaction product i is calculated as $Y_i = XS_i$. With respect to the values of $Y_{C=C}$, the catalysts follow the sequence PtKL > PtSrKL > PtLaKL > PtNdKL > PtSmKL, in parallel with the order of the corresponding conversions of citral in Fig. 3. So, PtKL is the most active hydrogenation catalyst and also the most active one for producing citronellal and their hydrogenated derivatives. In contrast, as shown in Fig. 6, all the doped catalysts are more active for producing geraniol and nerol than PtKL. It is remarkable, in this sense, that the values of $Y_{C=O}$ for PtSrKL and PtNdKL, after 100 min of reaction (10.0% and 9.9%, respectively) are twice that of PtKL (4.4%) while the respective overall conversions are lower, even less of one half in the case of PtNdKL.

It has been reported that zeolites containing well-defined and isolated Lewis acid sites seem to be the best heterogeneous catalysts in the Meerwein–Ponndorf–Verley reduction of aldehydes and the complementary Oppenauer oxidation of alcohols (MPVO) [46]. For that reason, in order to detect possible formation of unsaturated alcohols through that reaction mechanism, blank experiments were performed with the lanthanide promoted catalysts in the absence of hydrogen, at 323 K and 5 MPa. Under these conditions no unsaturated alcohols were observed and, hence, we believe that the enhancement of S_{G+N} observed in Fig. 4 for all the doped catalysts is kinetic in origin, which arises from the electronic modifications of platinum produced by the effect of either lanthanides or Sr, above explained. Electron-rich and electron-deficient species at the catalyst surface can promote the formation of unsaturated alcohols from citral following different mechanisms, in agreement with the theoretical approach by Delbecq and Sautet [47], either by inhibiting the hydrogenation of the C=C conjugated double bond and/or by favoring the hydrogenation of the C=O bond.

The evidenced kinetic effects can be explained with the help of the simplified reaction scheme in Fig. 7, where for the sake of simplicity only hydrogenation steps have been considered over the catalyst surface. The scheme shows the adsorption–desorption steps of reactants and products, with the activated intermediate species in the adsorbed phase (θ_i); K_i is the adsorption–desorption equilibrium constant for a product i and k_i the kinetic constant for a reaction step. Assuming that under our experimental conditions hydrogenation of the isolated C=C double bond and the other side reactions are negligible, as well as the hydrogenation steps are irreversible, the overall reaction rate constant k for the disappearance of citral under kinetic regime will be $k = k_1 + k_2$. As suggested, adsorption of citral (E + Z) on the catalyst surface occurs through either the C=C conjugated double bond or the C=O carbonyl group, with the subsequent formation of the respective activated complex in the adsorbed phase, whereas hydrogen chemisorbs and homolytically dissociates on Pt^0 [48] to give the adatoms Pt-H, (θH). Interaction of that reactive complex with two neighboring θH species leads to either the chemisorbed precursor of citronellal (θ_{Cal}) or the precursor of the unsaturated alcohols (θ_{G+N}). These adsorbed species can be either desorbed to the liquid phase as citronellal, geraniol and nerol or successively hydrogenated with and/or without any previous desorption to form the precursors of citronellol (θ_{Col}) and 3,7-dimethyloctanol ($\theta_{3,7DMO}$), which subsequently desorb to the liquid phase. Under these conditions electron-deficient metal species ($Pt^{\delta+}$) as well as electron-rich platinum species ($Pt^{\delta-}$) may substantially affect the adsorption

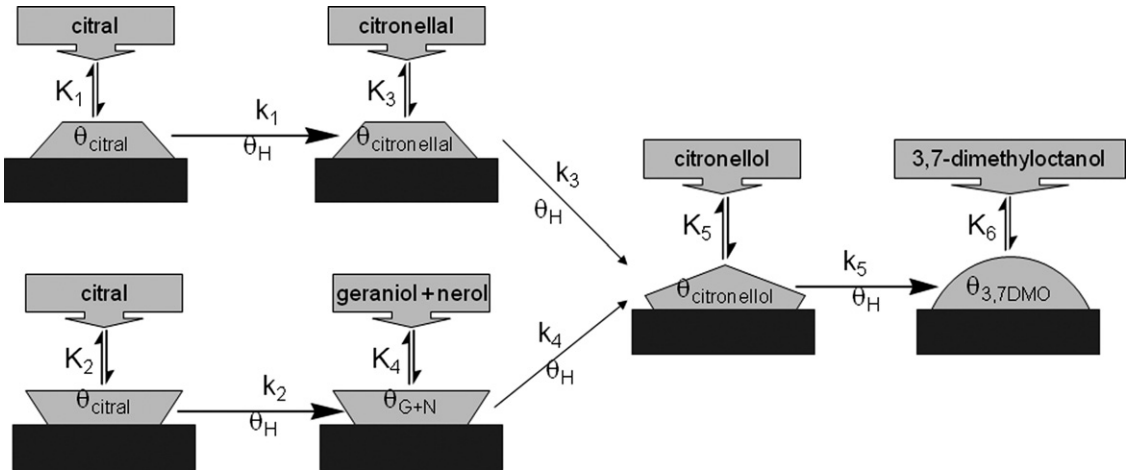

Fig. 7. Simplified reaction scheme for citral hydrogenation at the surface of Pt/KL catalysts in the liquid phase.

mode of citral and also the adsorption–desorption equilibrium constants of the intermediates and the kinetic constants of the different reaction steps, giving rise to catalytic performances very different to that of the parent catalyst, PtKL.

For catalysts containing lanthanides, Pt^0 species in association with $Pt^{\delta+}$ species located in the close proximity and in adequate proportion, can constitute active sites dual in nature [$Pt^{\delta+}$–Pt^0] which are particularly active for hydrogenation of the C=O group of the citral molecule. The positive effect of electron-deficient metal species on the formation of unsaturated alcohols in the hydrogenation of different α,β-unsaturated aldehydes has been treated in several reviews [49,50] and discussed by different authors [16,17]. In this sense, Bachiller-Baeza et al. [27] attributed the enhanced selectivity towards geraniol and nerol from citral over Fe–Ru catalysts to the polarizing effect of $Fe^{\delta+}$ species on the C=O bond. Recently [25] we have suggested that positively charged ionic species, in the surrounding of Ru^0, improve the activation of carbonyl bond over RuCu/KL catalysts. For bimetallic catalysts using Ge and Sn as promoter, it has been also reported enhanced activity for hydrogenation of carbonyl group of citral [8,9] and of other α,β-unsaturated aldehydes [44,51]. In all cases, stabilization of partially oxidized species ($Me^{\delta+}$) has been considered to be the origin of the carbonyl bond activation. Stabilization and association of both types of metal species, $Ru^{\delta+}$ and Ru^0, was also suggested in sulfurized Ru/KL catalysts, and their positive effect on the transformation of citral into unsaturated alcohols discussed [25]. Likewise, a positive effect of electron-deficient metal species ($Me^{\delta+}$) in coexistence with well reduced metal species (Me^0) has been proposed in the hydrogenation of aromatics [52], methylcyclopentane conversion [53] and in the hydrogenolysis of chlorocarbons [54] among other reactions. In our case, it is plausible that citral chemisorbs on the dual active site [$Pt^{\delta+}$–Pt^0] through the C=O group, in such a manner that carbon is anchored to the Pt^0 species, while the nucleophilic oxygen is bonded to an adjacent $Pt^{\delta+}$ species. This highly reactive intermediate complex is attacked by hydrogen homolytically dissociated on the surrounding Pt^0 sites, to form the adsorbed precursor of the unsaturated alcohols (θ_{G+N}). It is probable, on the other hand, that lanthanide countercations in association with Pt^0 species can also constitute active sites [$Me^{\delta+}$–Pt^0] thus contributing to the higher selectivity towards geraniol and nerol of these catalysts. The result will be that both K_2 and k_2, in Fig. 6, increase with respect to the counterparts for PtKL, while K_1 and k_1 diminish.

For PtSrKL, stabilization of electron-rich platinum species ($Pt^{\delta-}$) at the surface, favored by the high dispersion of SrO species, also modifies the adsorptive properties of the catalyst and the kinetic constants of the surface reactions with respect to those of PtKL. In this line, a positive effect was proposed for KOH in the hydrogenation of cinnamaldehyde and citral over Pt/carbon catalysts [55], for NaOH in the hydrogenation of cinnamaldehyde over Pt catalysts [56] and for other electron-donor systems in selective hydrogenation reactions [3]. Enhanced formation of geraniol and nerol over [$Pt^{\delta-}$–$Co^{\delta+}$] species in supported bimetallic Pt–CO catalysts has been also claimed [6]. In PtSrKL a high charge density on the metal surface atoms ($Pt^{\delta-}$) can decrease the binding energy of the C=C bond and, on the other hand, favor the back-bonding interactions with the $\pi^*_{C=O}$-orbital to a larger extent than with $\pi^*_{C=C}$-orbital and therefore the hydrogenation of the C=O bond with respect to that of C=C double bond [47]. As result, K_1 and k_1 will be diminished with respect to the corresponding values for PtKL, while formation of unsaturated alcohols will be indirectly improved. On the other hand, the transformation rate of citronellal into citronellol (k_3) is strongly enhanced in comparison to that of citral into citronellal, resulting in the rapid decrease of S_{Cal} in favor of S_{Col}, as the conversion increases.

4. Conclusions

Incorporation of rare earth as countercations, as well as an extraframework strontium oxide to KL zeolite, substantially modifies the surface properties that govern the behavior of Pt/KL supported catalysts in the hydrogenation of citral in the liquid phase. The partial substitution of K^+ by lanthanide ions increases the surface acidity of the catalysts, thus favoring the dispersion of the metal and the formation of electron-deficient platinum species ($Pt^{\delta+}$). In comparison with PtKL the overall hydrogenation activity of those catalysts is inhibited, but their respective activity for hydrogenation of the carbonyl group of citral is kinetically enhanced, increasing the selectivity towards geraniol + nerol from 6% to 32%. Strontium oxide in PtSrKL increases the basicity of the zeolite, hinders the dispersion of Pt, increases the stability of the catalyst and promotes the formation of electron-rich platinum species ($Pt^{\delta-}$). This latter inhibits the hydrogenation of the C=C conjugated double bond of citral, but improves that of the C=O bond and favors the successive hydrogenation of citronellal to citronellol, which reaches 80% selectivity at 60% conversion. Remarkably the electronic modifications of the Pt nanoparticles have been simultaneously detected by a spectroscopic technique (XPS) and by a catalytic test, such as the competitive hydrogenation of toluene/benzene mixtures.

Acknowledgements

Authors acknowledge the MICINN Spain (Projects CTQ-2008-06839-C03-01 and 03-PPQ) for the financial support.

References

[1] J. Kijenski, P. Winiarek, Appl. Catal. A: Gen. 193 (2000) L1–L4.
[2] Z. Poltarzewski, S. Galvagno, R. Pietropaolo, P. Staiti, J. Catal. 102 (1986) 190–198.
[3] P. Gallezot, D. Richard, Catal. Rev. Sci. Eng. 40 (1998) 81–126.
[4] P. Mäki-Arvela, J. Hájek, T. Salmi, D.Yu. Murzin, Appl. Catal. A: Gen. 292 (2005) 1–49.
[5] S. Galvagno, A. Donato, G. Neri, R. Pietropaolo, J. Mol. Catal. 49 (1989) 223–232.
[6] N.M. Bertero, A.F. Trasarti, B. Moraweck, A. Borgna, A.J. Marchi, Appl. Catal. A: Gen. 358 (1) (2009) 32–41.
[7] M. Englisch, V.S. Ranade, J.A. Lercher, J. Mol. Catal. A: Chem. 121 (1997) 69–80.
[8] T. Ekou, A. Vicente, G. Lafaye, C. Especel, P. Marécot, Appl. Catal. A: Gen. 314 (1) (2006) 73–80.
[9] A. Vicente, T. Ekou, G. Lafaye, C. Especel, P. Marécot, J. Catal. 275 (2) (2010) 202–210.
[10] S. Galvagno, A. Donato, G. Neri, R. Petropaolo, Catal. Lett. 8 (1991) 9–14.
[11] P. Claus, D. Hönicke, in: M.G. Scaros, M.L. Prunier (Eds.), Catalysis of Organic Reactions, Marcel Dekker, New York, 1995, pp. 431–433.
[12] E. Tronconi, C. Crisafulli, S. Galvagno, A. Donato, G. Neri, R. Pietropaolo, Ind. Eng. Chem. Res. 29 (1990) 1766–1770.
[13] S. Galvagno, A. Donato, G. Neri, R. Pietropaolo, J. Mol. Catal. 78 (1993) 227–236.
[14] B. Coq, P.S. Kumbhar, C. Moreau, P. Moreau, F. Figueras, J. Phys. Chem. 98 (1994) 10180–10188.
[15] P. Gallezot, A. Giroir-Fendler, D. Richard, Catal. Lett. 4 (1990) 169–174.
[16] D.G. Blackmond, R. Oukaci, B. Blanc, P. Gallezot, J. Catal. 131 (1991) 401–411.
[17] P. Gallezot, B. Blanc, D. Barthomeuf, M.I. Païs da Silva, Stud. Surf. Sci. Catal. 84 (1994) 1433–1438.
[18] D. Tas, R.F. Parton, K. Vercruysse, P. Jacobs, Stud. Surf. Sci. Catal. 105 (1997) 1261–1268.
[19] J. Hájek, N. Kumar, P. Mäki-Arvela, T. Salmi, D.Y. Murzin, I. Paseka, T. Heikkilä, E. Laine, P. Laukkanen, J. Väyrynen, Appl. Catal. A: Gen. 251 (2003) 385–396.
[20] J. Hájek, N. Kumar, P. Mäki-Arvela, T. Salmi, D.Y. Murzin, J. Mol. Catal. A: Chem. 217 (2004) 145–154.
[21] G.J. Li, T. Li, U.D. Xu, S.T. Wong, X.X. Guo, Stud. Surf. Sci. Catal. 105 (1997) 1203–1210.
[22] J. Álvarez-Rodríguez, I. Rodríguez-Ramos, A. Guerrero-Ruiz, A. Arcoya, Catal. Today 107–108 (2005) 302–309.
[23] J. Álvarez-Rodríguez, A. Guerrero-Ruiz, I. Rodríguez-Ramos, A. Arcoya, Micropor. Mesopor. Mater. 97 (2006) 122–131.
[24] J. Álvarez-Rodríguez, A. Guerrero-Ruiz, I. Rodríguez-Ramos, A. Arcoya, Micropor. Mesopor. Mater. 110 (2008) 186–196.
[25] J. Álvarez-Rodríguez, A. Guerrero-Ruiz, A. Arcoya, I. Rodríguez-Ramos, Catal. Lett. 129 (2009) 376–382.
[26] R.M. Tri, J. Massadier, P. Galezot, B. Imelik, Stud. Surf. Sci. Catal. 11 (1982) 141–148.
[27] B. Bachiller-Baeza, A. Guerrero-Ruiz, P. Wang, I. Rodríguez-Ramos, J. Catal. 204 (2001) 450–459.
[28] D.W. Breck, Zeolite Molecular Sieves, Structure, Chemistry and Use, Wiley & sons, New York, 1974, p. 113.
[29] M.M.J. Tracy, J.B. Higgins, R. Von Ballmoos, Zeolites 16 (1996) 734–735.
[30] M. Grau, L. Daza, X.L. Seoane, A. Arcoya, Catal. Lett. 53 (1998) 161–166.
[31] E.K. Rideal, Concepts in Catalysis, Academic Press, London, 1968, pp. 281–304.
[32] G. Larsen, G.L. Haller, Catal. Lett. 3 (1989) 103–110.
[33] T.T. Phuong, J. Massadier, P. Gallezot, J. Catal. 102 (1986) 456–459.
[34] W.M.H. Sachtler, A.Yu. Stakheev, Catal. Today 12 (1992) 283–295.
[35] T. Homeyer, Z. Karpinski, W.M.H. Sachtler, J. Catal. 123 (1990) 60–73.
[36] G. Jacobs, F. Ghadially, A. Pisanu, A. Borgna, W. Alvarez, D.E. Resasco, Appl. Catal. A: Gen. 188 (1999) 79–98.
[37] U.K. Singh, M.A. Vannice, J. Catal. 199 (2001) 73–84.
[38] P. Mäki-Arvela, N. Kumar, A. Nasir, T. Salmi, D.Yu. Murzin, Ind. Eng. Chem. Res. 44 (2005) 9376–9383.
[39] J. Álvarez-Rodríguez, I. Rodríguez-Ramos, A. Guerrero-Ruiz, A. Arcoya, Appl. Catal. A: Gen. 366 (2009) 114–121.
[40] M. Burgener, R. Wirz, T. Mallat, A. Baiker, J. Catal. 228 (2004) 152–161.
[41] P. Mäki-Arvela, N. Kumar, K. Eränen, T. Salmi, D.Yu. Murzin, Chem. Eng. J. 122 (2006) 127–134.
[42] U.K. Singh, M.N. Sysak, M.A. Vannice, J. Catal. 191 (2000) 181–191.
[43] U.K. Singh, M.A. Vannice, J. Catal. 191 (2000) 165–180.
[44] I.M.J. Vilella, S.R. de Miguel, C. Salinas-Martinez de Lecea, A. Linares-Solano, O.A. Scelza, Appl. Catal. A: Gen. 281 (2005) 247–258.
[45] F. Qin, W. Shen, C. Wang, H. Xu, Catal. Commun. 9 (2008) 2095–2098.
[46] A. Corma, M.E. Domine, L. Meneth, S. Valencia, J. Am. Chem. Soc. 124 (2002) 3149–3495.
[47] F. Delbecq, P. Sautet, J. Catal. 152 (1995) 217–236.
[48] S. Tsuchiya, Y. Amenomiya, R.J. Cvetanovic, J. Catal. 19 (1970) 245–255.
[49] P. Kluson, L. Cerveny, Appl. Catal. A: Gen. 128 (1995) 13–31.
[50] V. Ponec, Appl. Catal. A: Gen. 149 (1997) 27–48.
[51] P. Mäki-Arvela, L.P. Tiainen, M. Lindblad, K. Demirkan, N. Kumar, R. Sjöholm, T. Ollonqvist, J. Väyrynen, T. Salmi, D.Y. Murzin, Appl. Catal. A: Gen. 241 (2003) 271–288.
[52] M.V. Ramahan, A. Vannice, J. Catal. 127 (1991) 251–266.
[53] X. Bai, W.M.H. Sachtler, J. Catal. 129 (1991) 121–129.
[54] L.M. Gómez-Sainero, X.L. Seoane, J.L.G. Fierro, A. Arcoya, J. Catal. 209 (2002) 279–288.
[55] V. Satagopan, B. Sandalia, J. Chem. Technol. Biotechnol. 60 (1994) 17–21.
[56] W. Yu, Y. Wang, H. Liu, W. Zheng, J. Mol. Catal. A: Chem. 112 (1996) 105–113.